Protease-Catalyzed Hydrolysis of Substrate Mimetics (Inverse Substrates): A New Approach Reveals a New Mechanism[†,‡]

Michael Thormann, Sven Thust, Hans-Jörg Hofmann, and Frank Bordusa*

Institute of Biochemistry, Faculty of Biosciences, Pharmacy, and Psychology, University of Leipzig, Talstrasse 33, D-04103 Leipzig, Germany

Received December 2, 1998

ABSTRACT: Contrary to common protease substrates, the hydrolysis of 4-guanidinophenyl esters of the Boc-Xaa-OGp type by trypsin and trypsin-like proteases performs easily and independently of the structure and chirality of the acyl moiety. The hydrolysis of this new class of *substrate mimetics*, previously called *inverse substrates*, is enabled by the highly specific leaving group. However, the mechanism cannot be explained on the basis of the conventional binding model which defines the interactions between the protease and its substrate. Hydrolysis and aminolysis kinetics, protein−ligand docking, and molecular dynamics studies have been carried out in order to get insight into the catalytic mechanism which holds for these substrate mimetics. The experimental and theoretical results obtained for the serine protease trypsin suggest a novel extended kinetic model. It explains the hydrolysis of these types of protease substrates and accounts for the structural consequences for their aminolysis.

The hydrolysis of natural peptide and common ester substrates by serine and cysteine proteases such as trypsin, chymotrypsin, papain, and clostripain follows a well-known mechanism (*1*−*5*) (Scheme 1). Substrate binding leads to a tetrahedral transition state where the carbonyl oxygen of the scissile bond (the oxyanion) is fixed in the oxyanion hole by hydrogen bonding to the backbone amide groups of Ser195 and Gly193. Subsequently, the tetrahedral intermediate collapses, expelling the leaving group and the acylenzyme results. The deacylation step is initiated by the attack of water and takes place oppositely to the acylation step forming a second tetrahedral intermediate which transforms into the enzyme−product complex. Several X-ray structures of serine proteases with active-site peptide inhibitors confirm this model (ref *6* and references therein).

The structural requirement for a protease substrate is the presence of specific amino acids in the acyl moiety, for example L-Arg or L-Lys in the case of trypsin. However, it has been shown that also the leaving group has a certain influence on the activity of the protease. Therefore, an extension of the enzyme−substrate interactions toward the S′-subsites (nomenclature according to refs *7* and *8*) is useful to gain still higher specificities (*6*, *9*−*12*).

A very different approach is the design of a new class of substrates, originally developed as time-dependent irreversible inhibitors of trypsin and trypsin-like proteases that have a nonspecific acyl residue, but bear a highly specific leaving group. The first examples of such substrates were 4-amidino- and 4-guanidinophenyl esters, which are well hydrolyzed by these proteases independently of their acyl moiety (*13*, *14*). Furthermore, it was demonstrated that also derivatives of this ester type are capable to serve as artificial recognition sites mediating a specific hydrolysis by these enzymes (*15*−*17*). This class of substrates becomes highly interesting for the trypsin-catalyzed peptide bond formation because the protease function is independent of the acyl moiety (*18*−*21*). Recently, we described an extension of this approach to irreversible peptide segment condensations with other proteases and introduced the term *substrate mimetics* (*22*).

Up to now, it remains open which mechanism applies for the hydrolysis of these substrate mimetics. It is questionable whether the above-mentioned model which defines distinct areas on the enzyme that bind the acyl group (S-subsite) and the leaving group (S′-subsite) could be maintained (Figure 1). The elucidation and understanding of the hydrolysis mechanism of substrate mimetics needs a detailed knowledge of the enzyme−substrate interactions. To clarify the catalytic mechanism, X-ray structures of enzyme−substrate complexes would be helpful but are not easily accessible due to the low intrinsic stability of these ester substrates. In this paper, hydrolysis kinetics investigations of substrate mimetics of the Boc-Xaa-OGp type with trypsin and protein−ligand docking studies have been performed leading to an extended kinetic model which could be verified by molecular dynamics and aminolysis experiments.

MATERIALS AND METHODS

Materials. Boc-amino acids,[1] 4-aminophenol, DCC, DMAP, benzyl chloroformate (Z-chloride), *S*-methylisothiourea, bovine trypsin (TPCK-treated), and Tos were purchased from commercial sources. If not otherwise stated, all chemicals were of analytical grade. Solvents were purified and dried by conventional methods.

[†] This work has been supported by the Deutsche Forschungsgemeinschaft (Ja 559/9-1 and Innovationskolleg "Chemisches Signal und biologische Antwort") and the Fonds der Chemischen Industrie.

[‡] Dedicated to Prof. Dr. H.-D. Jakubke on occasion of his 65th birthday.

* To whom correspondence should be addressed. E-mail: bordusa@uni-leipzig.de. Fax: +49-0341-9736998. Phone: +49-0341-9736918.

10.1021/bi9828425 CCC: $18.00
Published on Web 04/16/1999

Scheme 1: Kinetic Model of a Protease-catalyzed Hydrolysis Reaction

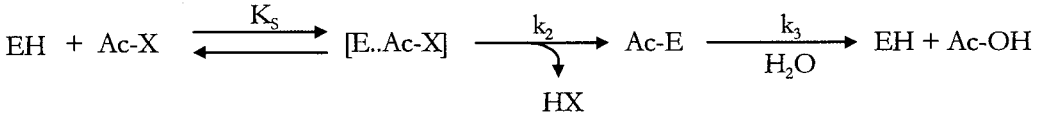

EH, free enzyme; Ac-X, substrate; [E···Ac-X], Michaelis−Menten complex; HX, leaving group; Ac-E, acylenzyme intermediate; Ac-OH, hydrolysis product.

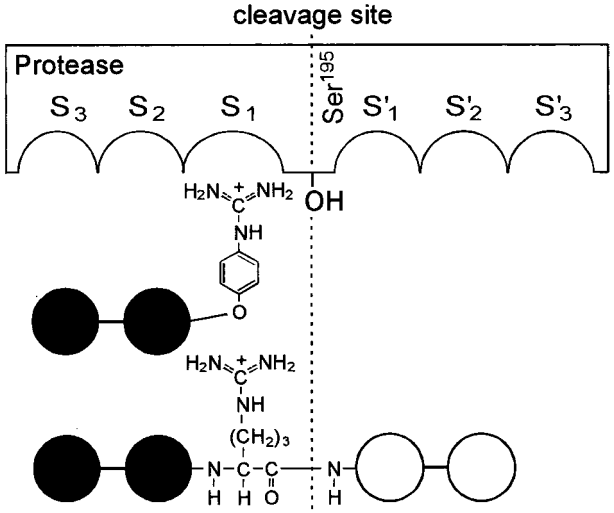

FIGURE 1: Schematic comparison of the binding of a substrate mimetic and a common peptide substrate to the active site of trypsin based on the ideas of the conventional binding model of proteases (nomenclature according to refs *7* and *8*).

Syntheses. N^{α}-*tert*-Butyloxycarbonyl amino acid 4-guanidinophenyl esters were prepared by condensation of the appropriate Boc-protected amino acid and 4-[*N*′,*N*″-bis(Z)-guanidino]phenol following the procedure described by Sekizaki et al. (*20*). Because of the more advantageous preparation and higher reactivity, *N*,*N*′-bis(Z)-*S*-methylisothiourea was used for the amidination of 4-aminophenol to synthesize 4-[*N*′,*N*″-bis(Z)guanidino]phenol (*23*) instead of 1-[*N*,*N*′-bis(Z)amidino]pyrazole. The benzoyl-protected esters Bz-Xaa-OGp(Z)$_2$ were prepared from the appropriate Boc-analogue by deprotection of the N^{α}-amino group with TFA and subsequently benzoylation using benzoyl chloride. A final catalytic hydrogenation of Bz-Xaa-OGp(Z)$_2$ and Boc-Xaa-OGp(Z)$_2$ results in the 4-N′,N″-deprotected derivatives. The reaction yields were between 65 and 85%. The identity and purity of the final products were checked by analytical HPLC at a wavelength of 220 nm, NMR, thermospray mass spectroscopy, and elemental analysis. In all cases, satisfactory elemental analyses data were found (±0.4% for C, H, N).

Hydrolysis Studies. All reactions were performed at 25 °C using an assay mixture containing 25 mM Mops buffer (pH 7.6), 0.1 M NaCl, 5 mM $CaCl_2$, and 20% methanol to realize complete solubility of the substrates. The substrate concentrations were between 0.006 and 2.0 mM and the enzyme concentrations between 6.3×10^{-9} and 1.0×10^{-7} M. The active enzyme concentration was determined by active-site titration using NPGB (*24*). The rate of reaction was analyzed by RP-HPLC determining the disappearance of substrate esters by at least 10 different concentrations. For this purpose, at defined time intervals, aliquots were withdrawn and diluted with a stop solution of 50% methanol containing 1% TFA. The kinetic parameters were analyzed by iterative nonlinear curve fitting of the untransformed data using the program SigmaPlot Scientific Graphic System (Vers. 1.01, Jandel Corp.). The values reported are the average of at least two independent experiments.

Aminolysis Studies. Enzymatic reactions were performed in a total volume of 60 μL containing 0.1 M Hepes buffer (pH 8.0), 0.2 M NaCl and 20 mM $CaCl_2$, at 25 °C. Stock solutions of substrates (4 mM) were prepared in water containing 10% DMF. Stock solutions of amino components (40 mM) were prepared in 0.2 M Hepes buffer (pH 8.0), 0.4 M NaCl and 40 mM $CaCl_2$. The final concentrations of substrate and amino component were 2 and 20 mM, respectively. The latter was calculated as free, N^{α}-unprotonated nucleophile concentration $[HN]_0$ according to the Henderson−Hasselbalch equation $[HN]_0 = [N]_0/(1 + 10^{pK-pH})$ (*25*). After thermal equilibration of the assay mixture, the reactions were initiated by the addition of 5 μL of enzyme stock solutions leading to enzyme concentrations between 1.0×10^{-6} and 1.25×10^{-4} M. At certain time intervals, 50 μL were withdrawn and diluted with 100 μL of stop solution containing 50% methanol and 1% TFA. For each substrate and amino component, an experiment without enzyme was carried out for determining the extent of nonenzymatic ester hydrolysis which was strictly less than 5%. On the basis of the same control experiments, nonenzymatic aminolysis of the substrate esters was investigated and could be ruled out. The partition values *p* reported are the average of at least three independent experiments.

HPLC Analyses. Samples were analyzed by analytical RP-HPLC using a C8 polymer-coated column [Grom Capcell, 5 μm, 300 Å (25 × 0.4 cm), Japan] and eluted with various mixtures of water/acetonitril containing 0.1% TFA under isocratic and gradient conditions. Detection was at 254 nm. The reaction rates and *p* values were calculated from the peak areas of the ester substrate, hydrolysis, and aminolysis products, respectively, with Tos as an internal standard.

Theoretical Calculations. The basis of the docking studies were the crystal structures 2ptn of bovine trypsin (*26*) and 2tgp of the trypsinogen−BPTI complex (*27*). All solvent molecules and ions were removed from the trypsin crystal structure. Trypsin and the ligand molecules Boc-Xaa-OGp were modeled with polar hydrogens and template charges using the Quanta96 program package (Molecular Simulations Inc., San Diego, 1996). For the docking calculations, the program AutoDock 2.41 (*28*), which successfully reproduces the crystal structures of nonflexible macromolecules with

[1] Abbreviations: Boc, *tert*-butyloxycarbonyl; BPTI, bovine pancreatic trypsin inhibitor; Bz, benzoyl; DCC, *N*,*N*′-dicyclohexylcarbodiimide; DMAP, 4-(dimethylamino)pyridine; DMF, dimethylformamide; Hepes, *N*-(2-hydroxyethyl)piperazine-*N*′-(2-ethanesulfonic acid); Mops, 3-(*N*-morpholino)propanesulfonic acid; NPGB, 4-nitrophenyl-4′-guanidinobenzoate; OEt, ethyl ester; OGp, 4-guanidinophenyl ester; TFA, trifluoroacetic acid; Tos, 4-toluenesulfonic acid; TPCK, *N*-tosylphenylalanine chloromethyl ketone; Xaa, individual amino acid; Z, benzyloxycarbonyl.

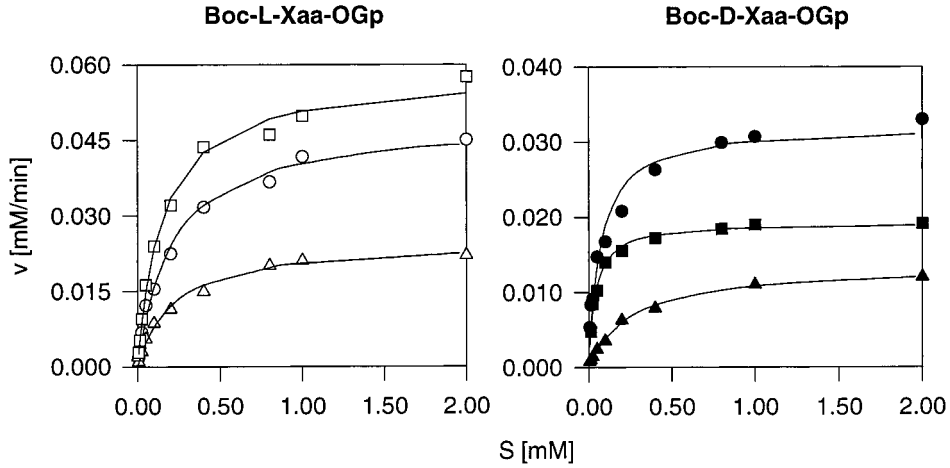

FIGURE 2: Plots of the initial rates of the tryptic hydrolysis of several Boc-Xaa-OGp substrates. (○) L-Ala; (△) L-Phe; (□) L-Leu; (●) D-Gln; (▲) D-Phe; (■) D-Glu. Conditions: 25 mM MOPS, pH 7.6, 0.1 M NaCl, 5 mM $CaCl_2$, 20% methanol, 25 °C. [Boc-Xaa-OGp]: 0.006−2.0 mM. [trypsin]: 6.3×10^{-9} to 1.0×10^{-7} M.

small flexible ligands (*29*), was employed. Recently, we have shown the applicability of this algorithm for trypsin complexes with peptide ligands (*30*). To allow the ligands searching the whole active site, a cubic box of 28 Å^3 was centered at Ser195 with a grid spacing of 0.22 Å. Each docking consisted of 20 runs, 50 cooling cycles, and at least 100 000 accepted or rejected steps per cycle resulting of about 100 000 000 trypsin−substrate arrangements in each calculation. The starting positions of the ligands were randomly chosen. Every new temperature cycle started from the lowest energy complex arrangement of the previous one. All relevant torsional angles were not restricted. According to the general ideas on the catalytic mechanism (*6*), those lowest-energy trypsin-Boc-Xaa-OGp complexes were the basis of all discussions which correspond to a productive orientation for catalysis, i.e., with the ester carbonyl oxygen in the oxyanion hole. On the basis of these complexes, acylated trypsins were modeled by removing the leaving group and forming the bond between Ser195 and the ester's carbonyl carbon. The CHARMm 23.1 force field was used (*31*). All residues within a radius of 5 Å around Ser195 were unconstrained. After energy minimization, heating, and equlilibration at 400 K, 4 ns gas-phase dynamics of Boc-L-Ala- and Boc-D-Ala-trypsin have been performed. The solvent accessibility of the carbonyl oxygen of Phe41 has been calculated for each sampled structure to see whether the S′- or the S-subsite was occupied by the acyl moiety.

RESULTS

The hydrolysis data were obtained performing trypsin-catalyzed steady-state kinetic studies with all substrate mimetics except the Arg-containing ones, which had to be excluded due to synthetic problems. Plots of the initial rates of hydrolysis for some derivatives are shown in Figure 2. All plots show the typical Michaelis−Menten kinetics without evidence of substrate inhibition or activation. The resulting kinetic data are listed in Table 2 and demonstrate that all substrates with L- and even those with D-amino acids are cleaved by trypsin. Analyzing the second-order rate constants k_{cat}/K_M for the Boc-Xaa-OGp substrates, the highest specificity is indicated for Xaa = L-Lys followed by L-Phe, Gly, L-Leu, L-Ala, L-Gln, and L-Glu. The D-amino acid analogues were found to be less specific by 1−2 orders of magnitude. This effect can directly be addressed to the decrease of the corresponding k_{cat} values (Table 2). In contrast, the K_M values are quite similar for the two enantiomeric series. Remarkably, in most cases the Michaelis constants are even slightly lower for the D-analogues.

Table 1: Calculated Binding Energies (kcal/mol) for the Most Stable Catalytically Productive Complexes of Boc-Xaa-OGp and Trypsin

substrate	ΔE_{tot}[a]	ΔE_{int}[b]	$\Delta\Delta E_{int}$[c]
Boc-L-Ala-OGp	−59.6	−70.1	9.0
Boc-D-Ala-OGp	−52.8	−59.5	19.6
Boc-Gly-OGp	−56.3	−64.5	14.6
Boc-L-Leu-OGp	−59.6	−65.2	13.9
Boc-D-Leu-OGp	−64.6	−69.9	9.2
Boc-L-Gln-OGp	−59.1	−68.3	10.8
Boc-D-Gln-OGp	−59.1	−68.3	10.8
Boc-L-Phe-OGp	−63.8	−67.7	11.4
Boc-D-Phe-OGp	−65.3	−70.7	8.4
Boc-L-Glu-OGp	−55.5	−63.4	15.8
Boc-D-Glu-OGp	−66.6	−69.3	9.8
Boc-L-Lys-OGp	−63.8	−79.1	0
Boc-D-Lys-OGp	−65.7	−73.4	5.7
Boc-L-Arg-OGp	−58.7	−70.3	8.8
Boc-D-Arg-OGp	−65.4	−75.0	4.2

[a] Total interaction energy of complex. [b] Intermolecular interaction energy. [c] Relative intermolecular binding energy.

Table 2: Steady-State Kinetic Parameters for the Hydrolysis of Boc-Xaa-OGp by Trypsin[a]

substrate	K_M (mM)	k_{cat} (s^{-1})	k_{cat}/K_M (M^{-1} s^{-1})
Boc-L-Ala-OGp	0.206	32.4	1.6×10^5
Boc-D-Ala-OGp	0.161	0.61	3.8×10^3
Boc-Gly-OGp	0.087	23.5	2.7×10^5
Boc-L-Leu-OGp	0.146	38.8	2.7×10^5
Boc-D-Leu-OGp	0.035	0.85	2.5×10^4
Boc-L-Gln-OGp	0.239	35.2	1.5×10^5
Boc-D-Gln-OGp	0.071	0.68	9.6×10^3
Boc-L-Phe-OGp	0.211	66.1	3.1×10^5
Boc-D-Phe-OGp	0.249	9.0	3.6×10^4
Boc-L-Glu-OGp	0.071	5.5	7.6×10^4
Boc-D-Glu-OGp	0.039	0.43	1.1×10^4
Boc-L-Lys-OGp	0.107	270	2.5×10^6
Boc-D-Lys-OGp	0.314	15.7	5.0×10^4

[a] Conditions: 25 mM Mops, pH 7.6, 100 mM NaCl, 5 mM $CaCl_2$, 25 °C; errors are less than 15%.

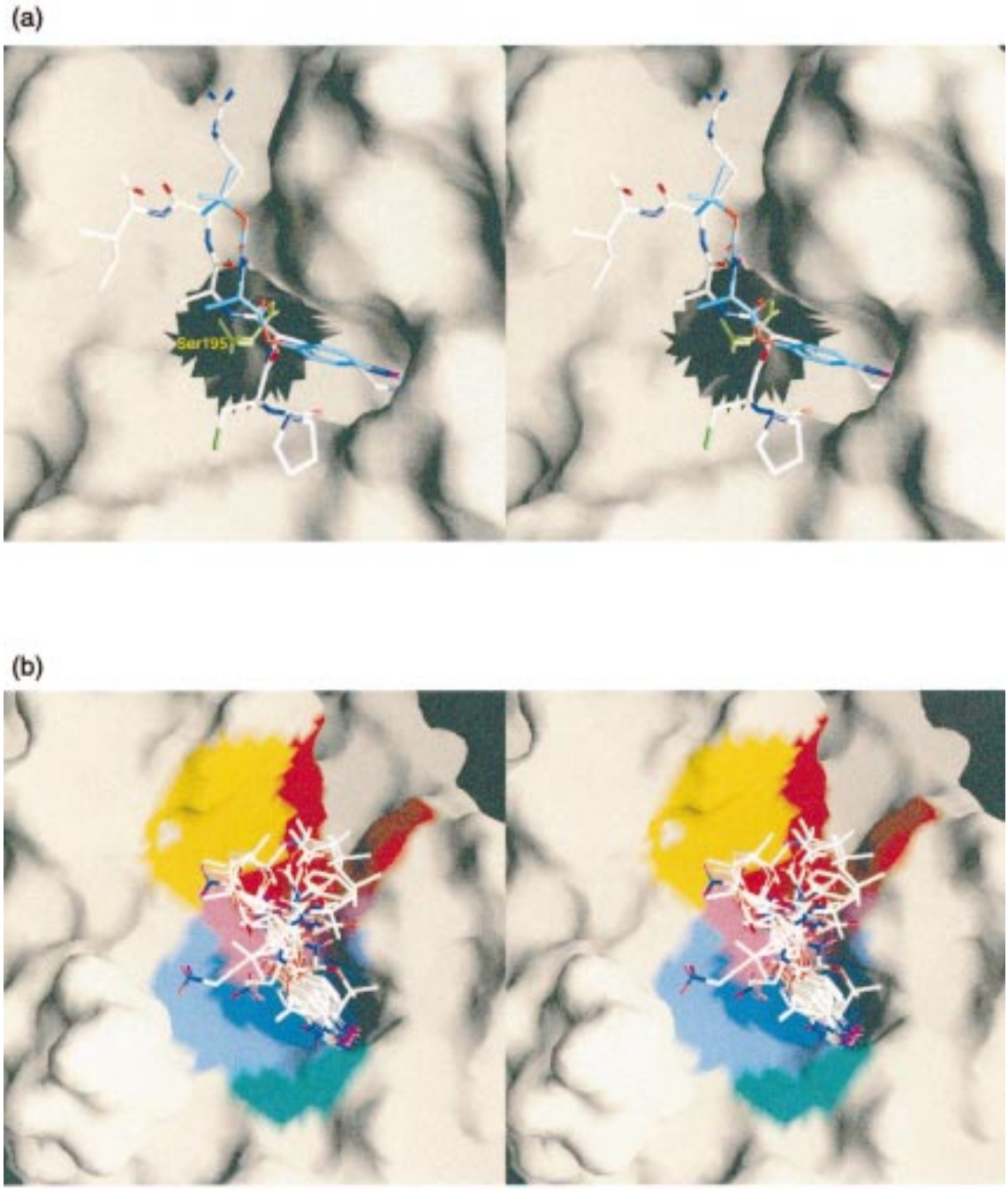

FIGURE 3: Binding of Boc-Xaa-OGp to trypsin as stereoview. (a) Comparison of the binding conformation of the P_3-P_3' residues of BPTI (Pro13-Cys14-Lys15-Ala16-Arg17-Ile18) and the lowest energy state of Boc-L-Ala-OGp to the active site of trypsin. BPTI (white); Boc-L-Ala-OGp (blue). (b) Calculated lowest-energy productive complexes of Boc-Xaa-OGp and trypsin. Xaa: Gly, L-Ala, D-Ala, L-Leu, D-Leu, L-Gln, D-Gln, L-Glu, D-Glu, L-Phe, D-Phe, L-Lys, and D-Lys. The regions of the subsites S_3 (green), S_2 (light blue), S_1 (blue), S_1' (pink), S_2' (red), and S_3' (orange) are also shown.

The binding of the substrate mimetic Boc-L-Ala-OGp, which bears an acyl residue unspecific for trypsin, has been simulated by its docking toward the active site of trypsin. All low-energy states found in the docking procedure exhibit the 4-guanidinophenyl group bound to the arginine-specific S_1-binding pocket. The enzyme−substrate interactions are comparable to the side chains of L-Arg and L-Lys due to the structural similarity of the leaving group. Obviously, the enzyme recognizes the substrate mimetic by the specificity-bearing leaving group and not by the acyl (peptide) moiety. A comparison between the binding of Boc-L-Ala-OGp and the P_3-P_3' residues of BPTI (Pro13-Cys14-Lys15-Ala16-Arg17-Ile18) is shown in Figure 3a.

The substrate specificity of the enzyme should be reflected by the calculated binding energies. Therefore, a representative set of Boc-Xaa-OGp substrate analogues was docked toward trypsin. Amino acids Xaa with positively and negatively charged as well as aromatic and aliphatic side chains were selected. Moreover, derivatives with L- and D-configuration at the C^α atom were considered. As calculated for Boc-L-Ala-OGp, all these substrates bind with their OGp leaving group in S_1 (Figure 3b). This holds even for the substrates Boc-L-Arg-OGp and Boc-L-Lys-OGp despite the presence of the S_1-specific arginine and lysine residues, thus indicating a higher S_1-specificity for 4-guanidinophenol. In each case, a productive binding conformation was found where the

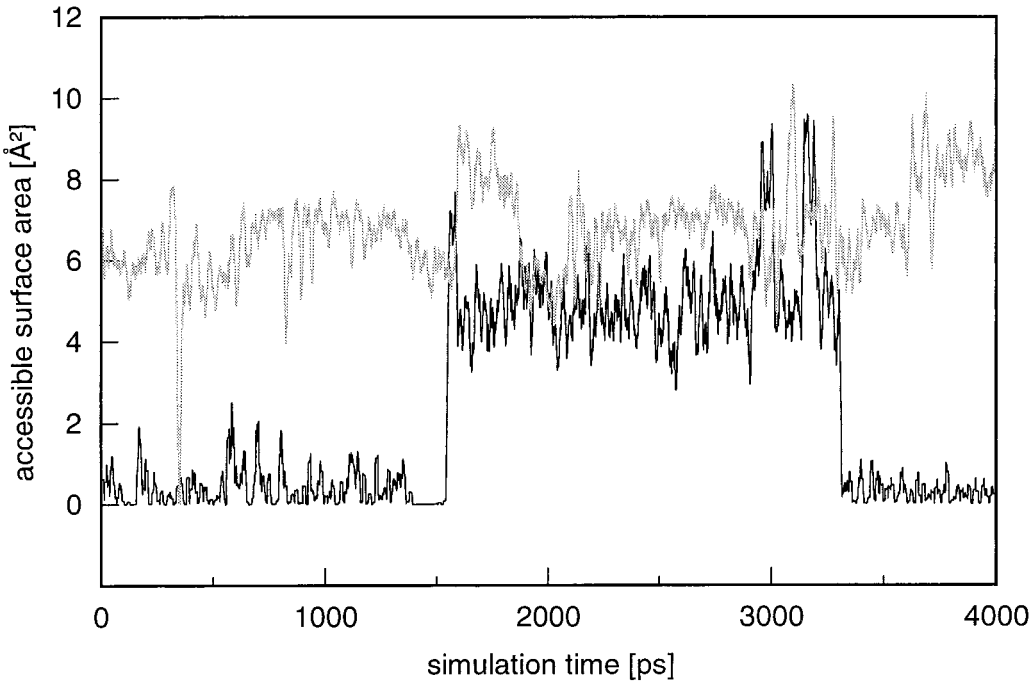

FIGURE 4: Plots of the water-accessible surface area of the Phe41 carbonyl oxygen from two gas-phase trajectories for Boc-L-Ala- (gray) and Boc-D-Ala-trypsin (black). Phe41 resides in the S_1'-region of the enzyme and, therefore, an occupied S′-site leads to drastically reduced accessibilities.

scissile ester bond is close to Ser195 as exemplarily indicated in Figure 3a. The binding energies of these conformations represent a measure for the specificity of trypsin toward these substrates. As shown in Table 1, the largest binding energy has been calculated for the L-Lys substrate followed by D-Arg, D-Lys, L-Arg, D-Phe, and L-Ala. The glutamic acid has the lowest affinity within the L-series. While the L-Ala substrate binds rather well, the D-analogue shows the lowest binding energy.

Because Boc-L-Ala- and Boc-D-Ala-substrates show the most striking differences, the dynamic behavior of their acyl-trypsins has been explored by molecular dynamics simulations. Both trajectories started with the acyl moiety in S′. However, a flip to the S-subsite has been observed in both cases (Figure 4). In the D-Ala complex, this takes about 1.5 ns, much more than in the L-Ala complex where the acyl residue flips already within the 300 ps equilibration period to its preferred site. In both cases, the backward flip has also been found, indicating a dynamic equilibrium between both states.

The aminolysis of the acylenzyme by added amino components is a convenient approach to investigate the S′-subsites of proteases. Therefore, aminolysis studies can provide information on the role of the S′-region in the cleavage of substrate mimetics. The efficiency of aminolysis and competitive hydrolysis of the acylenzyme can be quantified by the partition value *p* (*32*). This parameter is defined as the concentration of the amino component at which the rate of aminolysis reaction equals the rate of hydrolysis reaction. Using excess of the amino component, the *p* value can be calculated according to the equation $p =$ [Ac-OH]/([Ac-N][HN]), where [Ac-OH] corresponds to the hydrolysis product, [Ac-N] to the aminolysis product, and [HN] to the concentration of the amino component. The results of the aminolysis reactions with Bz-L-Ala-OGp, Bz-L-Leu-OGp, and their appropriate enantiomers using amino acid amides, di- and tripeptides as amino components are summarized in Table 3. The common substrate Bz-L-Arg-OEt was used as a reference. The *p* values indicate an aminolysis by the added amino components for all cases. With the exception of Bz-L-Ala-OGp, the ratios between hydrolysis and aminolysis were significantly lower for substrate mimetics than for the common substrates. All substrates including Bz-L-Arg-OEt show practically the same profile indicating similar interactions of the amino components with the various acylenzymes. In contrast, their absolute *p* values show partly remarkable differences. In the case of the Bz-L/D-Ala-OGp enantiomers, up to 80-fold lower *p* values for the deacylation of the D-configured derivative were observed. In a similar way the aminolyses of Bz-L/D-Leu-OGp were found to be catalyzed but the differences between the enantiomers were lower.

DISCUSSION

The most striking structural differences of the Boc-Xaa-OGp substrate mimetics to common peptide substrates are the nonspecific acyl residue and the highly specific leaving group. All L-amino acid derivatives are hydrolyzed despite the lacking trypsin-specific acyl moieties. Moreover, even the cleavage of D-amino acid derivatives performs easily. This shows clearly that substrate mimetics behave differently from common substrates. On the basis of the familiar model, conventional substrates bind with their acyl residue to the S-binding site of the enzyme having the leaving group at the S′-subsite and the scissile bond between attacked by Ser195. Applying the same binding principles for the acyl moiety of the substrate mimetics leads to a catalytically unproductive binding (Figure 1). The acyl residue would bind at the S-subsite of the enzyme, but the scissile bond would be far away from the active site and could not be attacked by Ser195. Hence, hydrolysis would not occur and, therefore,

Table 3: Partition Values for the Aminolysis of Boc-D/L-Ala-OGp and Boc-D/L-Leu-OGp Compared to the Common Substrate Bz-Arg-OEt by Trypsin[a]

	partition value p (mM)				
amino component	Bz-Arg-OEt	Bz-L-Ala-OGp	Bz-D-Ala-OGp	Bz-L-Leu-OGp	Bz-D-Leu-OGp
H-Met-NH_2	13.8	43.4	4.22	5.08	2.89
H-Leu-NH_2	21.2	72.2	6.16	15.5	10.3
H−Ser-NH_2	72.2	170	4.40	27.8	10.6
H-Gly-NH_2	124	130	6.90	69.1	15.2
H-Gln-NH_2	129	220	10.8	36.5	15.8
Ala-Arg	12.6	50.0	0.86	8.84	2.41
Ala-Met	39.4	104	1.70	20.6	3.90
Ala-Ala	24.6	121	2.03	14.7	3.97
Ala-Ser	74.4	388	9.36	71.9	20.1
Ala-Gly	154	564	14.4	86.2	30.6
Ala-Ala-Pro	12.2	35.2	0.82	7.40	1.62
Ala-Ala-Ala	20.4	71.2	0.88	9.10	2.26
Ala-Ala-Lys	23.4	74.2	0.96	8.60	2.64

[a] Conditions: 0.2 M Hepes, pH 8.0, 0.2 M NaCl, 20 mM $CaCl_2$, 25 °C. [substrate], 2 mM; [amino component], 20 mM; errors are less than 15%.

Scheme 2: Cartoon of the Extended Kinetic Model of a Protease-catalyzed Hydrolysis of Substrate Mimetics Introducing the Novel Rearrangement Equilibrium Constant K_R

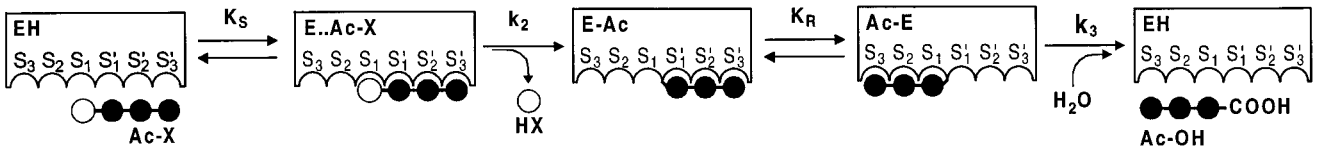

EH, free enzyme; Ac-X, substrate; [E···Ac-X], Michaelis−Menten complex; HX, leaving group; E-Ac, acylenzyme intermediate bearing the acyl residue at the S′-subsite; Ac-E, acylenzyme intermediate bearing the acyl residue at the S-subsite; Ac-OH, hydrolysis product.

cannot be explained on the basis of the conventional model of enzyme−substrate interaction.

The docking calculations convincingly show, however, that the specificity-bearing OGp group binds to the S_1-binding pocket like the L-Arg side chain of common peptide substrates. All substrate mimetics realize an arrangement where the scissile bond is very close to the hydroxy group of the active Ser195. As shown for Boc-L-Ala-OGp, the carbonyl group of the scissile ester bond is exactly located at the same position as the carbonyl group of the scissile peptide bond between P_1-Lys15 and P_1'-Ala16 in the trypsinogen−BPTI complex. This implies a possible attack by the enzyme which was confirmed by the hydrolysis studies. In contrast to common substrates, the acyl residues of these enzyme−substrate mimetic arrangements bind to the S′-subsite of trypsin (Figure 3). Thus, all binding sites beyond S_1 are only of minor importance for the recognition of these substrates. Therefore, the acyl residues of the substrate mimetics do not reflect the specificity of the S-binding site of the enzyme. Because the direction of the peptide backbone chain is reversed, the S′-subsite specificity is also not reflected. As a result, substrate mimetics show a unique specificity. This behavior of reversed recognition of substrate mimetics could also explain the effects found for peptide argininols of anisic acid of the general structure Y-$(Xaa)_n$-Arg-ψ-$(CH_2$-O)-CO-C_6H_4-OMe (Y = Boc, Ac) designed as time-dependent irreversible inhibitors of trypsin and trypsin-like proteases (*17*). To direct the homing of these derivatives to a special protease, the peptide sequence was mistakenly tuned to fulfill the individual S′-subsite specificity of the corresponding enzyme. Consequently, in most cases, the expected effect of selectivity for the corresponding protease could not be observed.

A correlation between the experimentally observed specificities expressed by the specificity constants k_{cat}/K_M of the hydrolysis kinetics and the theoretically calculated binding energies for the lowest energy enzyme−substrate complexes is possible on the basis of linear free energy relationships. Due to the distinct specificity constants, the data split up into two sets, the L-series including Gly and the enantiomeric D-series, respectively (Figure 5). Within each series, there is a good correlation between log k_{cat}/K_M and the binding energies. The substrates with the best binding energies are also the most specific ones. Interestingly, on one hand, the binding energies of the D-configured substrates are mostly lower than those for the somewhat weaker bound L-configured substrates. On the other hand, the D-configured substrates show distinctly lower specificity constants due to their lower k_{cat} values (Table 1) that reflect k_3 as the rate-limiting step of hydrolysis for this kind of substrates (*20*). An explanation for the low k_3 within the D-series provides

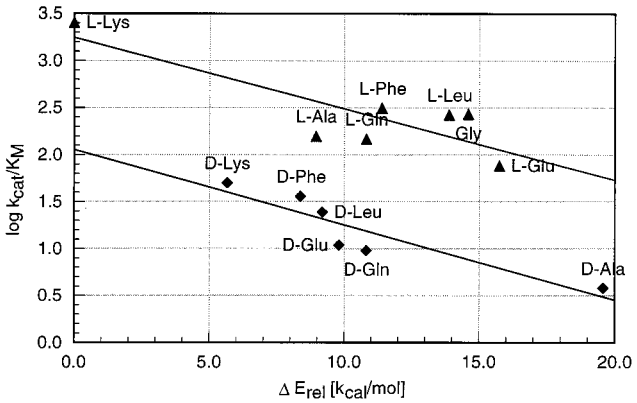

FIGURE 5: Correlation between the calculated binding energies of the most stable productive complexes of Boc-Xaa-OGp and trypsin and the specificity constants of the hydrolysis reaction. The correlation coefficients are $R = -0.84$ for the L-series including Gly (−▲−) and $R = -0.91$ (−◆−) for the D-series.

the detailed analysis of the catalytic mechanism. To perform the deacylation, it is of great importance that the acylated enzyme bears the acyl residue at the S-subsite. Thus, water can attack from the S′-side without hindrance. The acylation by a substrate mimetic, however, leads to an acylenzyme having the acyl residue at the S′-subsite of the enzyme which precludes the water attack. Hence, prior to the deacylation, the acyl residue has to flip to the S-subsite. Consequently, the kinetic model has to be extended by a rearrangement step between the two acylenzyme species E-Ac and Ac-E characterized by the equilibrium constant K_R (Scheme 2). The experimental findings show that D-configured substrates exhibit indeed lower k_{cat} values which might be related to lower K_R values. The high catalytic efficiency for L-configured substrates could be explained by significantly higher rearrangement equilibrium constants. To study the dynamic behavior of various acyl residues, their time-dependent occupancies in the S- and S′-subsites for Boc-L-Ala- and Boc-D-Ala-trypsin have been calculated. As illustrated in Figure 4, both the rearrangement step itself and the preferred binding of D-configured acyl residues to the S′-subsite and L-configured counterparts to the S-subsite could be confirmed.

For the experimental investigation of the S′-subsite accessibility, aminolysis studies are suitable. By their S′-specific binding, peptide nucleophiles should be able to push aside the acyl residue more efficiently from the S′-region than water. Therefore, the aminolysis of acyl enzymes bearing the acyl moiety in S′ should perform with higher rates than their hydrolysis. Consequently, the ratio of hydrolysis to aminolysis, as given by the *p* values, should be low for D-configured acyl residues and higher for the L-configured counterparts. The more their K_R values differ, the more their *p* values should vary. Indeed, the experimental results show dramatically lower *p* values for the deacylation of Bz-D-Ala- than for Bz-L-Ala-trypsin. In the case of the L-Leu and D-Leu analogues, the same situation occurs but with lower differences in the *p* values corresponding to the smaller differences in the hydrolysis kinetic constants (Table 2). The experimental results support a unique catalysis mechanism for substrate mimetics.

Finally, it can be concluded that the concept of substrate mimetics might be a general principle in enzyme catalysis which is not only restricted to trypsin and trypsin-like proteases.

ACKNOWLEDGMENT

We would like to thank Professor H.-D. Jakubke for inspiring discussions, Mrs. Doris Haines and Mrs. Regina Schaaf for skillful technical assistance.

REFERENCES

1. Bender, M. L., and Killheffer, J. F. (1973) *CRC Crit. Rev. Biochem. 1*, 149−199.
2. Rodgers, P. S., Goaman, L. C., and Blow, D. M. (1976) *J. Am. Chem. Soc. 98*, 6690−6695.
3. Kraut, J. (1977) *Annu. Rev. Biochem. 46*, 331−358.
4. Polgar, L. (1989) *Mechanisms of Protease Action*, CRC Press, Inc., Boca Raton.
5. Corey, D. R., McGrath, M. E., Vasquez, J. R., Fletterick, R. J., and Craik, C. S. (1992) *J. Am. Chem. Soc. 114*, 4905−4907.
6. Fersht, A. (1984*) Enzyme Structure* & *Mechanism*, 2nd ed., W. H. Freeman & Co., New York.
7. Schechter, I., and Berger, A. C. (1967) *Biochem. Biophys. Res. Commun. 27*, 157−162.
8. Schechter, I., and Berger, A. C. (1970) *Philos. Trans. R. Soc. London, B 257*, 249−264.
9. Fersht, A. R., Blow, D. M., and Fastrez, J. (1973) *Biochemistry 12*, 2035−2041.
10. Imperiali, B., and Abeles, R. H. (1987) *Biochemistry 26*, 4474−4477.
11. Butenas, S., Kalafatis, M., and Mann, K. G. (1997) *Biochemistry 36*, 2123-2131.
12. Ivanov, I. P., Yomtova, V. M., and Petkov, D. D. (1997) *Biocatal. Biotrans. 14*, 195−204.
13. Wagner, G., and Horn, H. (1973) *Pharmazie 28*, 428−431.
14. Tanizawa, K., Kasaba, Y., and Kanaoka, Y. (1977) *J. Am. Chem. Soc. 99*, 4484−4488.
15. Smith, R. A. G., Dupe, R. J., English, P. D., and Green, J. (1981) *Nature 290*, 505−508.
16. Been, M., de Bono, D. P., Muir, A. L., Bailton, F. E., Hillis, W. S., and Hornung, R. (1985) *Br. Heart J. 53*, 253−259.
17. Lynas, J. F., and Walker, B. (1997) *Bioorg. Med. Chem. Lett. 7*, 1133−1138.
18. Schellenberger, V., Jakubke, H.-D., Zapevalova, N. P., and Mitin, Y. V. (1991) *Biotechnol. Bioeng. 38*, 104−108, 319−321.
19. Mitin, Y. V., Schellenberger, V., Schellenberger, U., Jakubke, H.-D., and Zapevalova, N. P. (1991) in *Peptides 1990* (Giralt, E., and Andreu, D., Eds.) pp 287−288, ESCOM, Leiden.
20. Sekizaki, H., Itoh, K., Toyota, E., and Tanizawa, K. (1996) *Chem. Pharm. Bull. 44*, 1577−1579, 1585−1587.
21. Sekizaki, H., Itoh, K., Toyota, E., and Tanizawa, K. (1997) *Tetrahedron Lett. 38*, 1777−1780.
22. Bordusa, F., Ullmann, D., Elsner, C., and Jakubke, H.-D. (1997) *Angew. Chem., Int. Ed. Engl. 36*, 2473−2475.
23. Lal, B., and Gangopadhyay, A. K. (1996) *Tetrahedron Lett. 37*, 2483−2486.
24. Bergmeyer, H. U., Grassl, M., and Walter, H.-E. (1983) in *Methods of Enzymatic Analysis, Vol. II, Samples, Reagents, Assessments of Results* (Bergmeyer, H. U., Ed.) pp 319−320, Verlag Chemie, Weinheim.
25. Schellenberger, V., Könnecke, A., and Jakubke, H.-D. (1984) in *Peptides 1984* (Ragnarsson, U., Ed.) pp 201−204, Almqvist and Wirksell, Stockholm.
26. Walter, J., Steigemann, W., Singh, T. P., Bartunik, H., Bode, W., and Huber, R. (1982) *Acta Crystallogr., Sect. B 38*, 1462.
27. Huber, R., Bode, W., Deisenhofer, J., and Schwager, P (1983)- *Acta Crystallogr., Sect. B 39*, 480.
28. Goodsell, D. S., and Olson A. J. (1990) *Proteins: Struct., Funct., Genet. 8*, 195−202.
29. Morris, G. M., Goodsell, D. S., Huey, R., and Olson, A. J. (1996) *J. Comput.-Aided Mol. Des. 10*, 293−304.
30. Kurth, T., Grahn, S., Thormann, M., Ullmann, D., Hofmann, H.-J., Jakubke, H.-D., and Hedstrom, L. (1998) *Biochemistry 33*, 11434−11440.
31. Momany, F. A., Rone, R., Kunz, H., Frey, R. F., Newton, S. Q., and Schäfer, L. (1993) *J. Mol. Struct. (THEOCHEM) 286*, 1−18.
32. Schellenberger, V., and Jakubke, H.-D. (1991) *Angew. Chem., Int. Ed. Engl. 30*, 1437−1449.

BI9828425